Drag coefficient estimation of low density objects by free fall experiments

T. H. Günther[1,a)], K. A. Hoang[1,b)]

[1)]MCG Bönen, Billy-Montigny-Platz 5, 59199 Bönen, Germany

[a)]E-mail: dr.thomas.guenther@gmail.com
[b)]E-mail: khoihoang797@gmail.com

Published in Annals of West University of Timisoara - Physics, Vol. LXV, 2023

https://doi.org/10.2478/awutp-2023-0005

Abstract

The present article investigates whether the drag coefficient of low density objects can be determined by free fall experiments with sufficient accuracy. Among other things, the drag coefficient depends on the flow velocity, which can be controlled in wind channels experiments. Free fall experiments do not offer an experimental environment with constant flow velocity. Especially the later part of the movement gets relevantly influenced by air drag deceleration. We theoretically estimate an average sphere drag coefficient for the relevant part of the movement of falling spheres. The results are verified by examining the drag coefficient from experimental data. Finally, we determine the drag coefficient of a model rocket, which is compered to the result of the corresponding wind channel experiment.

1. Introduction

Air resistance can have significant influence on the motion of objects. The associated drag force depends on several properties, like geometry, mass, velocity and surface roughness of the object. Generally, the drag coefficient is measured in wind channels since it cannot be determined analytically. While wind channel experiments provide the possibility to preset a constant flow velocity, free fall experiments do not. Our aim is to estimate the air drag coefficient with a test setup that is as simple as possible. 1971 Lindemuth described a free fall experiment "*to measure the effect of air resistance on falling balls*" in [1]. "*The time of fall was measured* [...] *by using an array of mirrors to produce a ladder of light from a laser.* [...]". On the one hand, Lindemuth's experiment requires an elaborate experimental setup. On the other hand, he presupposes the air drag as $c_D \approx 0.5$ for Reynolds numbers $10^3 < R_e < 10^5$. Numerous publications are concerned with drag influence on free fall movements. Vial investigates the rise and fall of a mass in one dimension in the linear drag case, see [2]. Houari proposes "*a kinematic approach for measuring the drag coefficient of rotational symmetric objects falling through liquids* [...] *by numerically solving the equation of motion describing its fall through a known liquid contained in a vertical tube.*" [3]. During free fall in air, we have to deal with the quadratic drag case: "*At speeds less than about 1 m/s, the drag force on a sphere*

is proportional to the speed and is given by Stokes' law. At higher speeds, the drag force is proportional to the velocity squared and is usually small compared with the gravitational force if the object mass is large and its speed is low." [4]. In our paper we use a method similar to that given in [4] to estimate the air drag coefficient: The drop height and the falling time is measured. By solving the differential equation for free fall including air resistance, one gets the velocity and from this the vertical position of the object as a function of time. The drag coefficient of the falling object can be determined numerically from the zeros of this function. For the most part, the current article is concerned with the question how to interpret this result. Obviously the introduced method provides some kind of average drag coefficient which may correspond to an average flow velocity of the relevant part of the free fall. At the beginning, the velocity of the object is small and air drag negligible. But with increasing speed, drag force gets more and more influence. In order to be able to analyze our results, we first estimate the drag coefficient of spheres with our method. Adequate functions can be found in literature to describe the drag of a sphere as a function of the Reynolds number, see for example [5, 6]. We choose an approximation given in [5], which is valid up to $Re = 10^6$, to determine a constant average drag coefficient for the spheres. Therewith, one receives a suitable average drag coefficient which can be compared to the experimental result. Later we investigate whether the above mentioned method can be transferred to estimate the drag coefficient for other bodies. Therefore the drag coefficient of a model rocket is determined and compared to the results of a wind channel experiment. The results indicate, that this simple method is suitable for a rough drag coefficient estimation for low density objects.

2. Air resistance on free-falling objects

Air resistance is modeled by the drag force $F_D = \frac{1}{2}\rho_{\text{air}} c_D A_R v^2$, cf. [7, 6], where ρ_{air} is the density of the air, c_D the drag coefficient, A_R the reference area or characteristic area, and v the velocity of the object. For our concernes A_R can be choosen as the frontal area of the body, see [8, p.484]: "*Drag coefficients are defined by using a characteristic area A, which may differ depending on the body shape* [...]. *The area A is usually one of three types: 1. Frontal area, the body as seen from the stream; suitable for thick, stubby bodies, such as spheres, cylinders, cars, trucks, missiles, projectiles, and torpedoes.* [...]." If the falling object is a sphere with mass m, average density ρ_s and reference area $A_R = \pi r^2$, drag force causes the deceleration

$$a_D = \frac{F_D}{m} = \frac{\frac{1}{2}\rho_{\text{air}} c_D A_R v^2}{\rho_s V} = \frac{3\rho_{\text{air}} c_D v^2}{2\rho_s r} \propto \frac{c_D v^2}{\rho_s r}. \tag{2.1}$$

In order to get experimental data with sufficient accuracy, the influence of air drag must be noticeable. As it can be seen from (2.1), a_D increases for increasing velocity and drag coefficient or in case of decreasing average density ρ_s and radius of the sphere. Our aim is to determine the drag coefficient c_D, thus we can not adjust this parameter. The velocity v is bounded by the configuration of our experiment, i.e. it is limited by the height from which we are able to drop the object. The radius of the sphere has to be big enough for the video analysis. Hence, it is most feasible for us to choose a sphere with low average density in order to get evaluable data from our experiment. We compare our experimental data with theoretical approximations and try to transfer our method to other objects. In [5, p. 624] the drag coefficient of a sphere is modeled by

$$c_D\left(Re\right) = \frac{24}{Re} + \frac{2.6\left(\frac{Re}{5.0}\right)}{1+\left(\frac{Re}{5.0}\right)^{1.52}} + \frac{0.411\left(\frac{Re}{2.63\cdot 10^5}\right)^{-7.94}}{1+\left(\frac{Re}{2.63\cdot 10^5}\right)^{-8.00}} + \frac{0.25\left(\frac{Re}{10^6}\right)}{1+\left(\frac{Re}{10^6}\right)}, \tag{2.2}$$

see equation (8.83), which is "valid from the creeping-flow limit through $Re = 10^6$". The Reynolds number Re is determined by

$$Re = \frac{v\,L}{\nu} \tag{2.3}$$

where v is the velocity of the object, L its characteristic length, and ν the kinematic viscosity of the surrounding atmosphere, cf. [17, eq. 7.61]. The kinematic viscosity of air at $15°C$ is $\approx 1.5 \cdot 10^{-5} \frac{\mathrm{m}^2}{\mathrm{s}}$. NASA provides a "Similarity Parameter Calculator" which calculates the Reynolds number: https://www.grc.nasa.gov/www/k-12/airplane/viscosity.html.

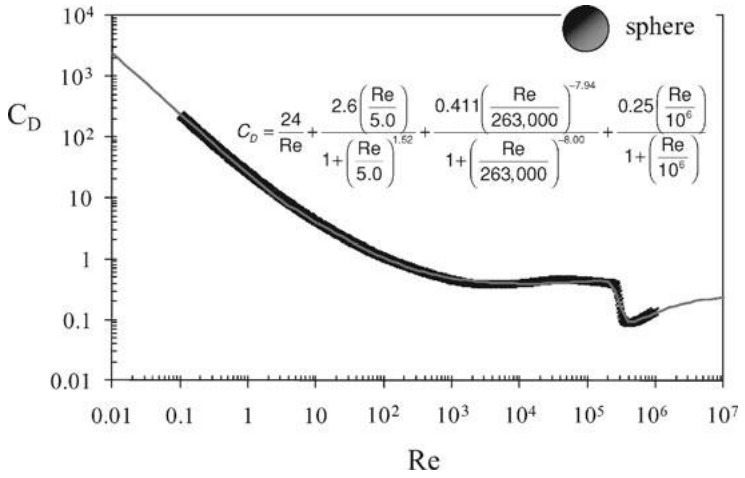

FIGURE 2.1. Sphere drag by (2.2) compared to experimental data, see [5, figure 8.13].

2.1. **Stokes drag.**

Objects that move very slowly through a fluid without generating turbulence are subject to Stokes' friction. In our case the fluid is the surrounding air. Drag force is approximately proportional to velocity:

$$F_D = -bv$$

The proportionality constant is the coefficient of viscosity, in case of small spherical objects $b = 6\pi\eta r$ where r is the radius and η is the fluid viscosity. The viscosity of air at $15°C$ is roughly $\eta \approx 1.8 \cdot 10^{-5} kg\, m^{-1} s^{-1}$. Further more, due to Archimedes' principle, an object submerged in a fluid experiences an upward buoyant force equal to the weight of the fluid displaced by the object. Let V be the volume of the falling sphere, ρ its density and ρ_{air} the density of air. The upward buoyant force $F_A = \rho_{\text{air}} V g$ acts against the force of gravity $F_G = mg = \rho V g$. The force approach results in $m\frac{dv}{dt} = F_G - F_A - F_D$ and we recieve the differential equation

$$\frac{dv}{dt} = \frac{(\rho - \rho_{\text{air}})\, Vg}{m} - \frac{6\pi\eta r}{m} v.$$

The corresponding integral equation

$$\int_0^t d\tau = \int_0^v \frac{dx}{\frac{(\rho-\rho_{\text{air}})Vg}{m} - \frac{6\pi\eta r}{m} x}$$

leads to the solution

$$v\,(t) = \frac{(\rho - \rho_{\text{air}})\, Vg}{6\pi\eta r} \left(1 - \exp\left(-\frac{6\pi\eta r}{m} t\right)\right). \tag{2.4}$$

From (2.4) one can easily compute the Reynolds number as a function of time, see (2.3).

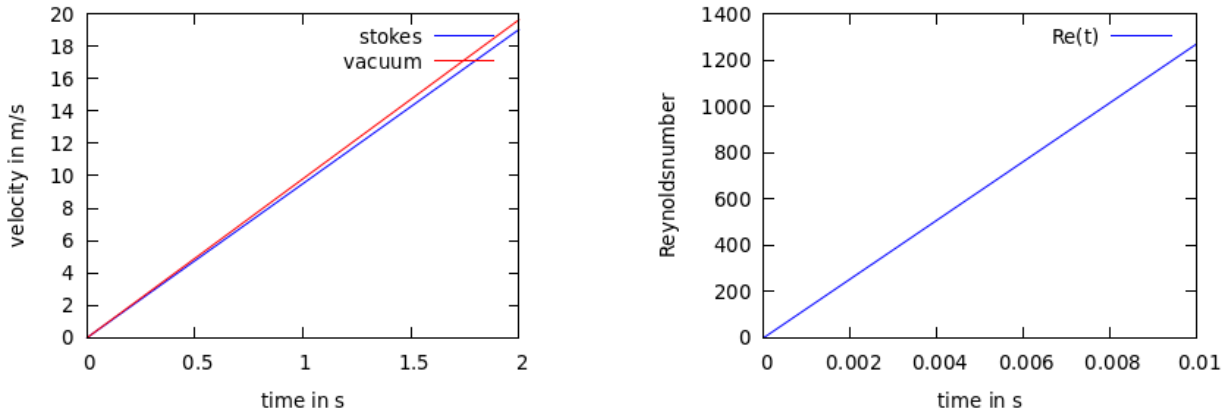

FIGURE 2.2. Free fall with Stokes friction for a sphere with radius $10\,cm$ and a mass of $169g$. Further parameters for air at $15°C$: viscosity $\eta \approx 1.8 \cdot 10^{-5} kg\,m^{-1}s^{-1}$, kinematic viscosity $\nu \approx 1.5 \cdot 10^{-5} \frac{\mathrm{m}^2}{\mathrm{s}}$ and density $\rho_{air} \approx 1.23\,kg\,m^{-3}$.

As can be seen from figure 2.2, the influence of Stokes friction can be completely neglected in our case. On one hand, within the first 2 seconds, there is hardly any deviation in the velocity of the fall compared to the fall in a vacuum. On the other hand, the Reynolds number exceeds 10^3 after 10 milliseconds which is the time measurement uncertainty in our experimental setup due to technical limitations. As a result, the range in which we are dealing with Stokes friction is so small that it falls below our measurement capabilities. Figure 2.2 was created with wxMaxima, for the sourcecode see https://github.com/tguent/airdrag_by_freefall.git.

As can be inferred from equation (2.3), a model that neglects Stokes friction loses its applicability for very small objects. While the Reynolds number still increases proportionally with the falling velocity, a small characteristic length ensures that the increase occurs much more slowly. Accordingly, small particles fall at lower Reynolds numbers, where Stokes friction has a significant impact on the motion of the fall. For this case, reliable alternatives are needed, such as a model in which the falling motion is evaluated piecewise. With that, the initial phase of the falling motion, where the Stokes friction dominates, can also be incorporated into the modeling. However, the falling motion of very small objects is indeed influenced by even the slightest air movements. This effect can be clearly observed, for example, in dust particles, which sometimes even seem to float in the air. Since our simple experimental setup can only be applied to small objects to a limited extent, we will omit such a piecewise model within the scope of this article. Therefore, we will restrict our experiment to objects of low density and with a sufficiently large reference area. Specifically, we will focus on spheres with small masses and adequately large radii.

2.2. **Velocity and distance for constant drag coefficient.**

Consider a free falling object with mass m. The object is dropped from height h at $t = 0$ with zero initial speed. Let us adopt the abbreviation

$$\psi = \frac{\rho_{\mathrm{air}}\, c_D\, A_R}{2m} \tag{2.5}$$

from [9]. Additionally, we consider c_D to be constant, therefore ψ is also a constant. Therewith the deceleration due to air drag takes the form $a_D = \psi v^2$. Gravity and drag force point in the opposite direction which leads to

$$\frac{dv}{dt} = g - \psi v^2 \tag{2.6}$$

The corresponding integral equation $\int_0^t d\tau = \int_0^v \frac{dx}{g-\psi x^2}$ has the solution

$$v\left(t\right) = \sqrt{\frac{g}{\psi}} \tanh\left(\sqrt{\psi g}\, t\right), \tag{2.7}$$

cf. [10]. Equation (2.7) can be integrated by substitution of $\xi = \cosh\left(\sqrt{\psi g}\, \tau\right)$ to receive the vertical position:

$$s\left(t\right) = \sqrt{\frac{g}{\psi}} \int_0^t \tanh\left(\sqrt{\psi g}\, \tau\right) d\tau = \frac{1}{\psi} \ln\left(\cosh\left(\sqrt{\psi g}\, t\right)\right). \tag{2.8}$$

In our case, the movement stops when the body hits the ground. Then $s\left(t\right)$ has reached the drop height h. If the free fall phase is long enough, a falling body reaches its terminal velocity v_∞ when the air resistance force becomes equal to the weight force. From (2.7) one gets

$$v_\infty = \lim_{t\to\infty} \left[\sqrt{\frac{g}{\psi}} \tanh\left(\sqrt{\psi g}\, t\right)\right] = \sqrt{\frac{g}{\psi}} = \sqrt{\frac{2mg}{\rho_{\text{air}}\, c_D\, A_R}}. \tag{2.9}$$

2.3. **Velocity for changing drag coefficient.**

As mentioned above, free fall experiments do not provide an experimental environment with constant flow velocity. The drag coefficient is actually a function that depends on the Reynolds number. The following considerations demonstrate that despite this, we still receive very good results using an approximation with a constant drag coefficient within our experimental framework. Following [5, p. 624], the function $cD\left(Re\right)$ for the drag coefficient of a falling sphere can be estimated by (2.2). Combination of (2.3), (2.5), (2.6) and (2.2) yields

$$\frac{dv}{dt} = g - \frac{\rho_{\text{air}}\, A_R}{2m} \left[cD\left(\frac{vL}{\nu}\right)\right] v^2.$$

In this model, the fall occurs towards increasing values along the vertical axis. We obtain the following two models for comparison

$$\frac{dv}{dt} = g - \frac{\rho_{\text{air}}\, A_R}{2m} \left[\frac{24\nu}{vL} + \frac{2.6\left(\frac{vL}{5.0\nu}\right)}{1+\left(\frac{vL}{5.0\nu}\right)^{1.52}} + \frac{0.411\left(\frac{vL}{2.63\cdot 10^5\nu}\right)^{-7.94}}{1+\left(\frac{vL}{2.63\cdot 10^5\nu}\right)^{-8.00}} + \frac{0.25\left(\frac{vL}{10^6\nu}\right)}{1+\left(\frac{vL}{10^6\nu}\right)}\right] v^2 \tag{2.10}$$

$$v\left(t\right) = \sqrt{\frac{g}{\psi}} \tanh\left(\sqrt{\psi g}\, t\right). \tag{2.11}$$

We solved equation (2.10) numerically with the Runge Kutta Algorithm. A wxMaxima code is provided here https://github.com/tguent/airdrag_by_freefall.git. The following considerations demonstrate that when choosing an appropriate constant drag coefficient in (2.11), both curves hardly differ from each other. The value of this drag coefficient can be determined from the terminal velocity (2.9) by

$$c_D = \frac{2mg}{\rho_{\text{air}}\, A_R\, v_\infty^2}. \tag{2.12}$$

The code is also included in the above mentioned wxMaxima file. As an example, the Runge Kutta Algorithm for (2.10) with the parameters $r = 10\,cm$, $m = 169\,g$, $\rho_{air} = 1.23\,kg\,m^{-3}$ and $\nu = 1.5 \cdot 10^{-5} m^2 s^{-1}$ outputs a terminal velocity of $v_\infty \approx 14.12\,m\,s^{-1}$. Equation (2.12) leads to $cD \approx 0.43$.

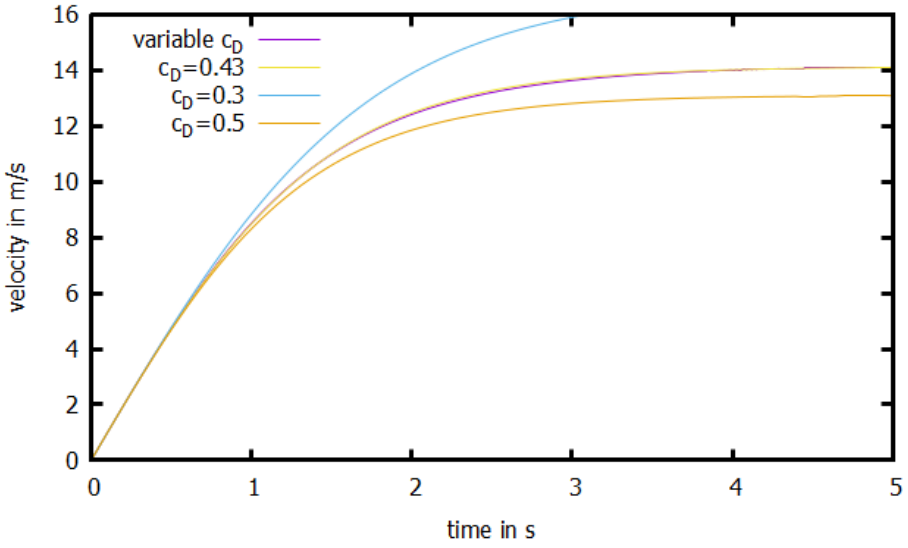

FIGURE 2.3. Velocity of the falling sphere given by (2.10) and velocity of the falling sphere modelled with constant drag coefficients given by equation (2.7).

Figure 2.3 shows the fitting of the solutions for the above mentioned parameters. Due to the good agreement, a mean value for cD can be obtained. For the sphere this is $cD = 0.43$.

2.4. **Influence of air drag within the experimental framework.**

Let $v_{air}(t)$ denote the falling velocity including air drag, see equation (2.7):

$$v_{air}(t) = \sqrt{\frac{g}{\psi}} \tanh\left(\sqrt{\psi g}\, t\right). \tag{2.13}$$

We compare (2.13) to the velocity $v_{vac}(t) = gt$ of a free falling object in a vacuum. Therewith we can calculate the difference of velocity $\Delta_{av}(t) := v_{vac}(t) - v_{air}(t)$ and define the function

$$D_v(t) := \frac{\Delta_{av}(t)}{v_{air}(t)} = \frac{gt - \sqrt{\frac{g}{\psi}} \tanh\left(\sqrt{\psi g}\, t\right)}{\sqrt{\frac{g}{\psi}} \tanh\left(\sqrt{\psi g}\, t\right)}. \tag{2.14}$$

Later we use the latter function D_v to gain some insights at which point the air drag becomes relevant for our concerns. Furthermore the free fall time in vacuum case $t_{vac} = \sqrt{2hg^{-1}}$ is a lower limit to the free fall time t_{air} with air resistance. Although it is not necessary to calculate the time t_{air}, since it is measured in our experiment, it can be easily obtained from (2.8). The object hits the ground at $s(t_{air}) = 0$ and therefore we get

$$t_{air} = \frac{1}{\sqrt{\psi g}} \text{Arcosh}\left(e^{\psi h}\right). \tag{2.15}$$

Interestingly, t_{vac} is the first order Taylor approximation of t_{air}. It is

$$t_{air} = \frac{1}{\sqrt{\psi g}} \text{Arcosh}\left(e^{\psi h}\right) = \sqrt{\frac{2h}{g}}\left(1 + \frac{\psi}{6}h + \mathcal{O}\left(h^2\right)\right) = t_{vac}\left(1 + \frac{\psi}{6}h + \mathcal{O}\left(h^2\right)\right). \tag{2.16}$$

For our concerns it is advantageous to compare the measured time t_{air} with the lower limit t_{vac} in order to early detect measurement error. To get an impression of how air resistance affects our experiment, we evaluate the function (2.14). Here we give an example: Consider a ball with a mass of $169g$ and radius of $0.1m$. This data roughly corresponds to Object B, see figure (3.1). Based on the considerations above, we estimated the drag coefficient of a ball of this size to 0.43, see section 2.3. That allows us to get an impression of the impact that air resistance will have on the ball in our experiment. Figure (2.4) shows the function (2.14) for the above data.

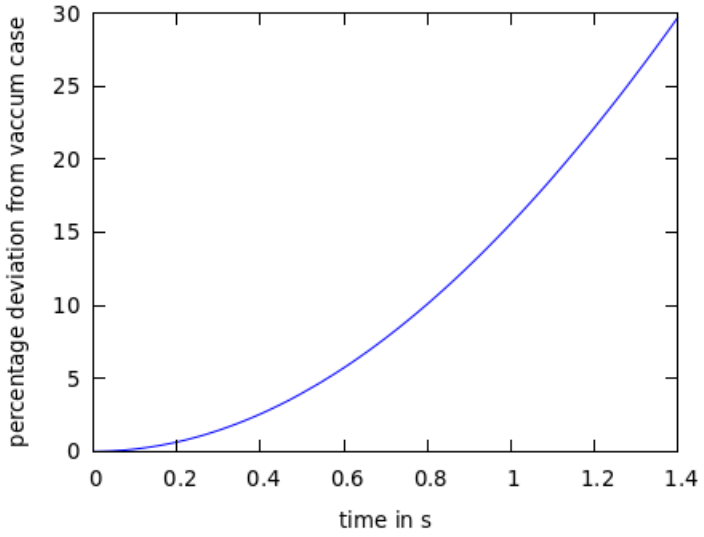

FIGURE 2.4. Function $100Dv\,(t)$ shows the percentage deviation of free fall with air drag from vacuum case for a sphere with radius $10\,cm$, mass of $169\,g$ and drag coefficient $c_D = 0.43$ for the first 1.4 seconds of free fall.

When the sphere hits the ground in our case (at $t = 1.38s \pm 0.01s$), the deviation due to air drag is in the range of 30%. The corresponding calculations were done by the computer algebra system wxMaxima [11]. The corresponding source code is available at https://github.com/tguent/airdrag_by_freefall.git.

3. The Experiment

For our experimental data we dropped seven different balls and a model rocket, see figure 3.1, from a height of $8.4m \pm 0.1m$. The drag coefficient of the model rocket is already known from previous research [9], where Prof. Dr. Andreas Brümmer kindly provided us the opportunity to determine the drag coefficient in a wind tunnel at TU Dortmund University.

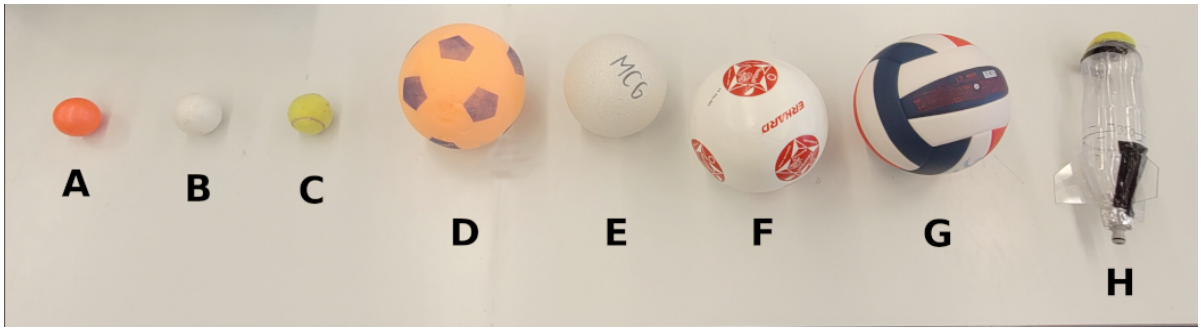

FIGURE 3.1. Objects

3.1. **Determination of air drag coefficient from experimental data.**

A simple method to get at least some kind of average drag coefficient is to calculate it from (2.15). Obviously, we receive the same result directly from equation (2.8) with $s\left(t_{air}\right)=0$, it is $\psi^{-1}\ln\left(\cosh\left(\sqrt{\psi g}\,t_{air}\right)\right)=h$. Nevertheless, the equation in either form cannot be solved analytically. With the hyperbolic cosine and the definition

$$f\left(\psi\right):=\exp\left(\sqrt{\psi g}\,t_{air}\right)+\exp\left(-\sqrt{\psi g}\,t_{air}\right)-2\exp\left(\psi h\right) \tag{3.1}$$

where $\psi=\rho_{\text{air}}\,c_D\,A_R m^{-1}/2$, cf. (2.5), the equation can be written in the form $f\left(\psi\right)=0$. This equation can be solved numerically with the Newton–Raphson method. The corresponding algorithm is implemented in the computer algebra system wxMaxima [11], available at https://github.com/tguent/airdrag_by_freefall.git. The measurement inaccuracies of ψ can be calculated from $t_{air}=\left(\psi g\right)^{-1/2}\operatorname{Arcosh}\left(e^{\psi h}\right)$, see (2.15). From the Gaussian error propagation law

$$\Delta t_{air}=\sqrt{\left(\frac{\partial t_{air}}{\partial\psi}\Delta\psi\right)^2+\left(\frac{\partial t_{air}}{\partial h}\Delta h\right)^2}$$

one gets

$$\Delta\psi=\sqrt{\left(\frac{\partial t_{air}}{\partial\psi}\right)^{-2}\left[\left(\Delta t_{air}\right)^2-\left(\frac{\partial t_{air}}{\partial h}\Delta h\right)^2\right]}$$

Together with

$$\frac{\partial t_{air}}{\partial\psi}=\frac{he^{\psi h}}{\sqrt{\psi g\left(e^{2\psi h}-1\right)}}-\frac{\operatorname{Arcosh}\left(e^{\psi h}\right)}{2\sqrt{\psi^3 g}}\quad\text{and}\quad\frac{\partial t_{air}}{\partial h}=\frac{\psi e^{\psi h}}{\sqrt{\psi g\left(e^{2\psi h}-1\right)}}$$

we finally receive for the error of ψ

$$\Delta\psi=\sqrt{\left(\frac{he^{\psi h}}{\sqrt{\psi g\left(e^{2\psi h}-1\right)}}-\frac{\operatorname{Arcosh}\left(e^{\psi h}\right)}{2\sqrt{\psi^3 g}}\right)^{-2}\left[\left(\Delta t_{air}\right)^2-\left(\frac{\psi e^{\psi h}}{\sqrt{\psi g\left(e^{2\psi h}-1\right)}}\Delta h\right)^2\right]} \tag{3.2}$$

The above formula allows for the indirect calculation of the Gauss error. Contrary to the usual addition of squares in the formula for Gaussian error, algebraically, a negative sign appears inside the square brackets under the square root. It is open for discussion whether this sign should be adjusted accordingly in order to calculate the maximum error. But this would be inconsistent with the algebraic transformations. Therefore, it is mathematically more consistent to calculate the error using the first-order Taylor expansion from (2.16). If one neglects the higher-order terms, the result is $t_{air}\approx t_{vac}\left(1+\frac{\psi}{6}h\right)$ with $t_{vac}=\sqrt{\frac{2h}{g}}$. Thus, we obtain

a formula,

$$\psi \approx \sqrt{\frac{18g}{h^3}} t_{air} - \frac{6}{h},$$

that allows us to calculate the Gauss error of psi directly. With

$$\frac{\partial \psi}{\partial t_{air}} = \sqrt{\frac{18g}{h^3}} \text{ and } \frac{\partial \psi}{\partial h} = -\sqrt{\frac{81g}{2h^5}} t_{air} + \frac{6}{h^2}$$

it remains

$$\Delta\psi = \sqrt{\frac{18g}{h^3}\left(\Delta t_{air}\right)^2 + \left(\frac{6}{h^2} - \sqrt{\frac{81g}{2h^5}} t_{air}\right)^2 \Delta h^2} \tag{3.3}$$

The drag coefficient c_D can be determined from equation (2.5)

$$c_D = \frac{2m\psi}{\rho_{\text{air}} A_R} \tag{3.4}$$

and its error is again calculated using the Gaussian error propagation law

$$\Delta c_D = \sqrt{\left(\frac{2m}{\rho_{\text{air}} A_R}\Delta\psi\right)^2 + \left(\frac{2\psi}{\rho_{\text{air}} A_R}\Delta m\right)^2 + \left(-\frac{2m\psi}{\rho_{\text{air}} A_R^2}\Delta A_R\right)^2}.$$

Using again (3.4) one receives

$$\Delta c_D = c_D \sqrt{\left(\frac{\Delta\psi}{\psi}\right)^2 + \left(\frac{\Delta m}{m}\right)^2 + \left(\frac{\Delta A_R}{A_R}\right)^2} \tag{3.5}$$

In case of a falling sphere with radius r, the reference area is $A_R = \pi r^2$. This leads to an error for the reference area of $\Delta A_R = 2\pi r \Delta r$ which can be implemented in (3.5). In the following, we will first provide a detailed example using Object D, cf. figure 3.1. The remaining results for the spherical objects are listed in the table below. Ball D has a mass of $169g \pm 1g$. Its circumference could be measured with an accuracy of about $3mm$. We received a radius of $0.1 \pm 5 \cdot 10^{-4} m$ from this. The time of the movement was measured by 210 fps slow motion video analysis with a results of $1.38s \pm 0.01s$, as we presume that there is an inaccuracy of one frame at the start and at the end of the movement in this case. As mentioned above, the falling height was $8.4m \pm 0.1m$. The air density (at a temperature of about $15°C$) is roughly $1.23\,kg\,m^{-3}$. With the above introduced method we receive for object D the drag coefficient $c_D = 0.34 \pm 0.06$. Interestingly, the error calculation using (3.3) yields $\Delta c_D \approx 0.0646$, a similar magnitude as calculating an upper error bound using the algebraically inconsistent sign change in equation (3.2), which leads to $\Delta c_D \approx 0.0629$. Only the algebraically consistent and exact version, with the unchanged equation (3.2), yields a significantly smaller error $\Delta c_D \approx 0.0199$. In summary, it can be concluded that the error calculated through Taylor expansion, using equation (3.3), appears to be the most suitable for providing an upper error bound in this context.

3.1.1. *The rocket's drag coefficient.*

The model rocket was made from a 1-liter plastic bottle which has a radius of $4\,cm$. The empty rocket has a mass of $143g$. We estimated the time for the $8.4m \pm 0.1m$ free fall to $1.35s \pm 0.01s$. The characteristic length lies in the range of $0.35m$, cf. [9]. This leads to an upper limit for the Reynolds number of roughly

Object	mass in g	radius in cm	falling time in s	drag coefficient c_D	c_D from theory
A	72 ± 1	3.3 ± 0.05	1.25 ± 0.01	N/A	0.402
B	154 ± 1	3.7 ± 0.02	1.23 ± 0.01	N/A	0.404
C	56 ± 1	3.3 ± 0.05	1.31 ± 0.01	0.04 ± 0.18	0.402
D	169 ± 1	10 ± 0.05	1.38 ± 0.01	0.34 ± 0.06	0.429
E	155 ± 1	7.9 ± 0.1	1.40 ± 0.01	0.63 ± 0.10	0.422
F	342 ± 1	10.4 ± 0.05	1.33 ± 0.01	0.19 ± 0.11	0.431
G	267 ± 1	10.3 ± 0.1	1.37 ± 0.01	0.43 ± 0.10	0.431

TABLE 1. Experimental results for the objects in figure 3.1. There are differences in measurement errors of the radius due to the different stability of the objects.

$3 \cdot 10^5$. Numerical evaluation of (3.1) leads to a drag coefficient of

$$c_D = 1.04 \pm 0.39$$

The error interval includes the more precise result of $c_D = 0.6 \pm 0.2$ from the wind tunnel measurement, see cf. [9]. One reason why a higher drag coefficient was measured in our experiment could be attributed to the fact that the rocket falls partially at a slight angle during free fall, resulting in a different angle relative to the flow. As a result, this could increase the effective reference area and alter its shape. In an improved experimental setup, it could be investigated whether there are ways to stabilize the angle of descent of the rocket, such as by attaching a small mass that can be later accounted for in the analysis.

3.2. **Analysis of measurement uncertainties.** As one can see, the deviations of the drag coefficient can be quite big with deviations up to the drag coefficient itself. Our measurement errors for height, radius, fall time, and mass yield an upper and a lower limit for the drag coefficient. Of course, Δc_D depends on the above mentioned measurement errors. The following considerations are intended to show the limitations of our experimental setup with regard to the density of the test objects. For this purpose, we are investigating how the error of the drag coefficient changes when only the mass of the object or only the radius is varied. It is not surprising that a change in the radius also affects Δc_D, since this changes the relative error of the radius. Same holds for the mass. But by doing so, we can try to get an idea of the range in which our method provides sufficiently accurate results.

Figure 3.2 shows that our experimental setup is not very suitable for spheres with a small radius, since the error scales with r^{-2}. Thus it is recommended to use bigger spherical objects. But on the other hand, one has to keep the mass of the objects in mind: Graph 3.3 shows how the error depends on the mass.

Obviously, our experimental setup is not suitable for determining the aerodynamic drag coefficient of heavy objects. In combination with the above considerations concerning the radial dependence of the error one

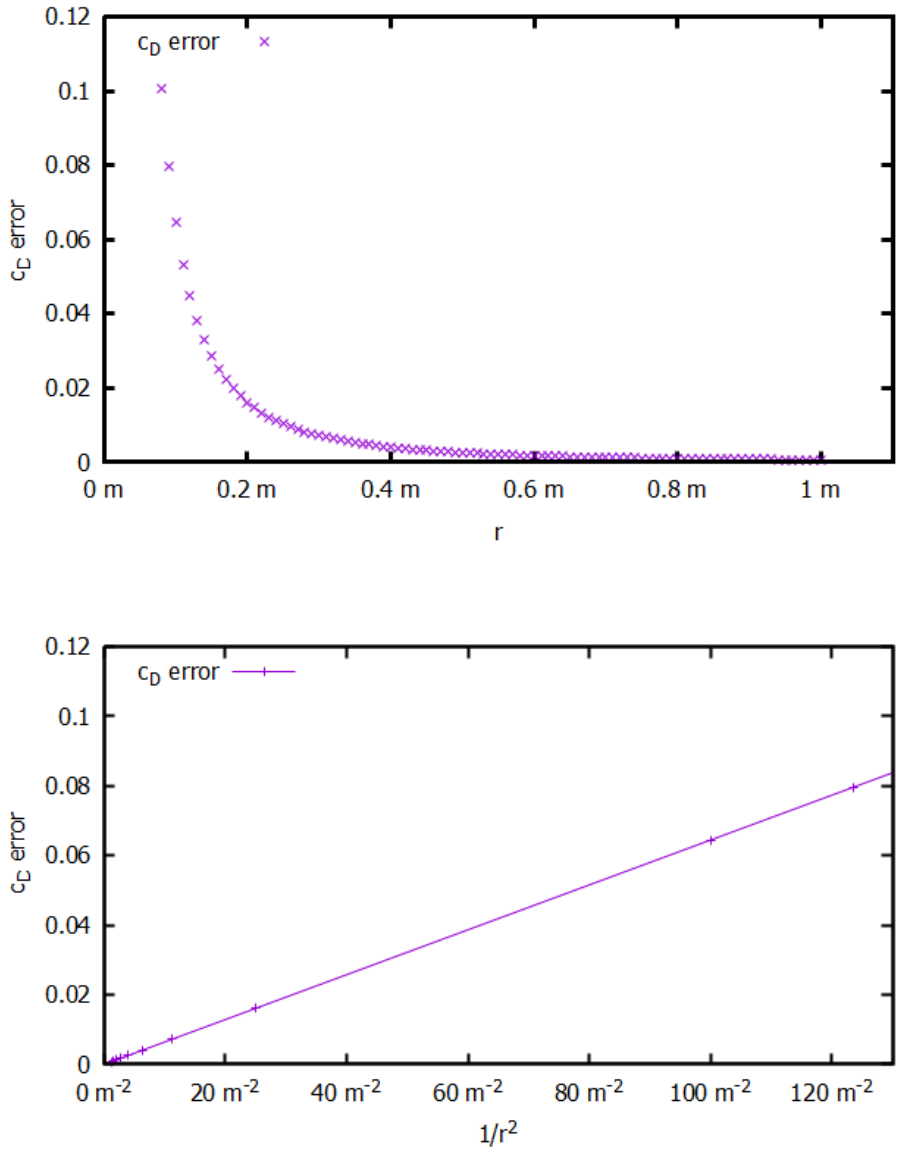

FIGURE 3.2. Error of drag coefficient for different radii and $m = 0.169\,kg$. Similarly, the height and the fall time remain the same. The graph indicates that $\Delta c_D \propto r^{-2}$.

can conclude that our experimental setup is recommended to be used for spheres with low masses and high radii, ergo for spheres with low densities. The relative error for the spheres with low densities tend to have a smaller relative drag coefficient error than spheres with bigger densities, see table 2:

It is noticeable that the measured value of the drag coefficient of the tennis ball (object C) in our experiment deviates significantly both from the theoretically calculated value and from the value measured in [12, see fig. 2]. As a rough rule of thumb, it can be inferred that our experimental setup is suitable for spheres with

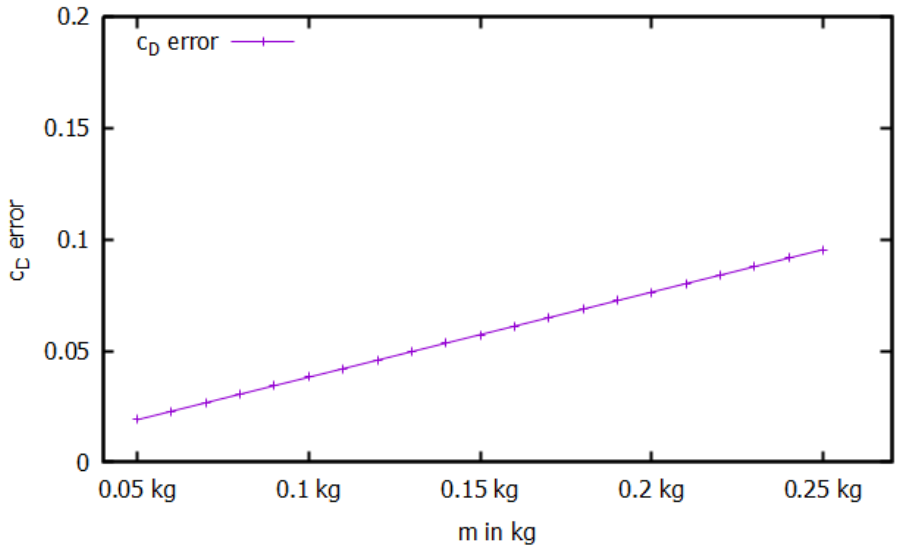

FIGURE 3.3. Error of drag coefficient for different masses and $r = 0.1m$. The graph indicates that $\Delta c_D \propto m$.

	average density ρ in $\frac{\text{kg}}{\text{m}^3}$	ratio ρ/ρ_{air}	upper limit Re	drag coefficient c_D	Δc_D in percent
A	478.30	389	$5.6 \cdot 10^4$	N/A	N/A
B	725.82	590	$6.3 \cdot 10^4$	N/A	N/A
C	372.01	302	$5.6 \cdot 10^4$	0.04 ± 0.18	225%
D	40.35	33	$1.7 \cdot 10^5$	0.34 ± 0.06	8.82%
E	75.05	61	$1.4 \cdot 10^5$	0.63 ± 0.10	17.46%
F	72.58	59	$1.8 \cdot 10^5$	0.19 ± 0.11	26.32%
G	58.33	47	$1.8 \cdot 10^5$	0.43 ± 0.10	9.30%
H	143	116	$3.0 \cdot 10^5$	1.04 ± 0.33	37.50%

TABLE 2. density as a multiple of the ambient density

low density up to roughly 100 times the air density. Even for the rocket, whose density is 116 times that of the surrounding density, the drag coefficient can be determined with our experiment. As expected, the error is larger compared to measurements in a wind tunnel.

4. Conclusion

As this study shows, estimation of the air drag coefficient by free fall experiments is suitable for rough approximations. It just needs a simple setup consisting of a camera and video cutting tools. We analyzed the data using the open source computer algebra system wxMaxima. Our error analysis shows, that this method gives good results for objects with low density up to about 100 times the air density. These results are in the range of the average drag coefficients in theory. For objects whose density is several hundred times that of the surrounding density, our experiment fails due to measurement inaccuracy. However, the experiment could be improved by using higher camera resolution and suitable slow-motion techniques. We investigated different balls as well as a D.I.Y model rocket, whose drag coefficient was previously determined in a wind tunnel. To sum up, this study shows that it is possible to estimate drag coefficients for low density objects that are topologically similar to a sphere with simple methods. Errors can be minimized by using objects with big reference areas and low masses.

References

[1] J. Lindemuth: The effect of air resistance on falling balls, Am. J. Phys. 39, 757–9 , 1971

[2] A. Vial: Fall with linear drag and Wien's displacement law: approximate solution and Lambert function, Eur. J. Phys. 33, 751, 2012

[3] A. Houari: Determining the drag coefficient of rotational symmetric objects falling through liquids, Eur. J. Phys. 33, 947, 2012

[4] R. Cross, C. Lindsey: Measuring the Drag Force on a Falling Ball, The Physics Teacher 52, 169, 2014; DOI: 10.1119/1.4865522

[5] A. Morrison, An Introduction to Fluid Mechanics, Cambridge University Press, New York, 2013

[6] P. Timmerman, J. P. van der Weele : On the rise and fall of a ball with linear or quadratic drag, American Journal of Physics 67 (6), 1999

[7] H. Stöcker, Taschenbuch der Physik, Verlag Harri Deutsch, Frankfurt am Main, 1998, ISBN 3-8171-1556-3

[8] F. M. White: *Fluid Mechanics*, McGraw-Hill, ISBN 978-0-07-352934-9, seventh edition, 2011

[9] L. Fischer, T. Günther, L. Herzig, T. Jarzina, F. Klinker, S. Knipper, F. G. Schürmann, M. Wollek, "Approximation of D.I.Y. Water Rocket Dynamics Including Air Drag," International Journal of Scientific Research in Mathematical and Statistical Sciences, Vol.6, Issue.6, pp.1-13, 2019. https://www.isroset.org/pdf_paper_view.php?paper_id=1620&1-IJSRMSS-02725-114.pdf

[10] I. N. Bronstein: *Taschenbuch der Mathematik*. B.G.Teubner Stuttgart-Leipzig, ISBN-3-8154-2001-6, 1996

[11] A. Vodopivec: wxMaxima 18.02.0. http://andrejv.github.io/wxmaxima/

[12] R. Mehta, F. Alam, A. Subic: Review of tennis ball aerodynamics, Sports Technology. 1:1, 7-16, DOI: 10.1080/19346182.2008.9648446, 2008